Achievable System Performance Gains Using Distributed Antenna Deployments

Martin Kurras, Kai Börner, Lars Thiele, Michael Olbrich and Thomas Haustein
Fraunhofer Institute for Telecommunications
Heinrich Hertz Institute
Einsteinufer 37, 10587 Berlin, Germany
martin.kurras@hhi.fraunhofer.de

***Abstract*—Heterogeneous networks (HetNets) using distributed antenna systems (DASs) have emerged as a promising candidate for future wireless cellular networks. In general by employing a DAS one places more remote radio units (RRUs) in a cell with one or more antennas to enhance coverage and capacity. These RRUs are connected to a central base band unit (BBU) via a high capacity and low latency connection. This paper shows achievable performance gains by deploying a DAS while keeping the number of transmit antennas the same as in a centralized antenna system (CAS). The proposed DAS architecture is an extension of a standard long term evolution (LTE) deployment. Performance evaluation is carried out by extensive system level simulations.**

***Index Terms*—DAS, HetNet, LTE-A, downlink, OFDMA**

I. Introduction

One of the greatest challenges of future wireless networks is the exponentially growing traffic demand [1], which can hardly be met with the current LTE CAS infrastructure. Therefore, the focus of research in the international community is shifted from a homogeneous to a heterogeneous network (HetNet) perspective. This means, e.g. to put additional antennas into an existing deployment to enhance system performance. In literature, e.g. [2], [3] and [4] DAS is considered as one of the candidates for HetNet. In a DAS the cell is covered by a number of distributed antennas and RRUs which are connected to a central BBU. Assuming the number of antennas being the same as in an equivalent LTE-CAS scenario the achievable system performance can be improved [5] or simply by adding more RRUs into the system [6]. In this work we focus on a DAS architecture with restriction to the current LTE infrastructure and include an extended more realistic antenna pattern compared to the International Telecommunications Union (ITU) recommended pattern from [7].
The paper is organized as follows. In Section II the deployment of the distributed antennas is presented. In Section III transmission concepts for our proposed DAS setup are described. Section IV describes the antenna configuration of the additional RRUs as well as the motivation for the usage of more realistic antenna patterns. Section V provides a brief description of the downlink system model. Detailed simulation parameters as well as the evaluation of the transmission strategies by means of system level simulations is presented in section VI. Finally, conclusions and a discussion of related problems are given in Section VII.

II. Distributed Antenna System

Consider the standard 3rd generation partnership project (3GPP) homogeneous urban-macro scenario case 1 from the system-simulation reference scenarios in [8] with an inter-site distance (ISD) of 500m where all antennas belonging to a single sector are located at a single eNodeB, henceforth labeled as LTE-CAS scenario. Within this work we extend this basic scenario by dropping new RRUs at the intersection of 3 sectors equidistant to eNodeBs from LTE-CAS, which seems a natural choice. Keeping in mind the overall restriction that the total number of transmit antennas should be the same as in the LTE-CAS scenario we place the fourth RRU in the center of the sector assuming a single antenna at each RRU, illustrated in Figure 1. As it can be seen, RRUs at the sector boarders are considered as sector antennas and the center antenna as an omni-directional radiator. In case that all RRUs are equipped with their own BBU a splitting of the original cell into 4 small cells is achieved. We refer to this scenario as LTE-dense because of the cell densification. If antennas related to one cell are connected to a central BBU e.g. by optical fiber, we call this scenario DAS.

III. Transmission Concepts

Three transmission concepts are described in the following Section. The antenna selection (AS) and single frequency network (SFN) modes are considered when all distributed antennas are connected to the same BBU and use the same cell id are explained in Subsection III-A and III-B. If each RRU is equipped with a its own BBU transmitting independently from each other, the LTE-dense concept is applied described in III-C.

A. Antenna Selection

The AS mode offers the user equipment (UE) the possibility to adaptively choose a number of streams or in other words the rank of the transmission. Single-AS refers to a transmission using a single antenna while a multi-AS stands for a transmission of two or more antennas. In the case of multi-AS multi-user (MU) multiple-input multiple-output (MIMO) is allowed. Figure 2 shows an illustration of the AS scheme rank 1.

978-1-4673-2569-1/12/$31.00 ©2012 IEEE

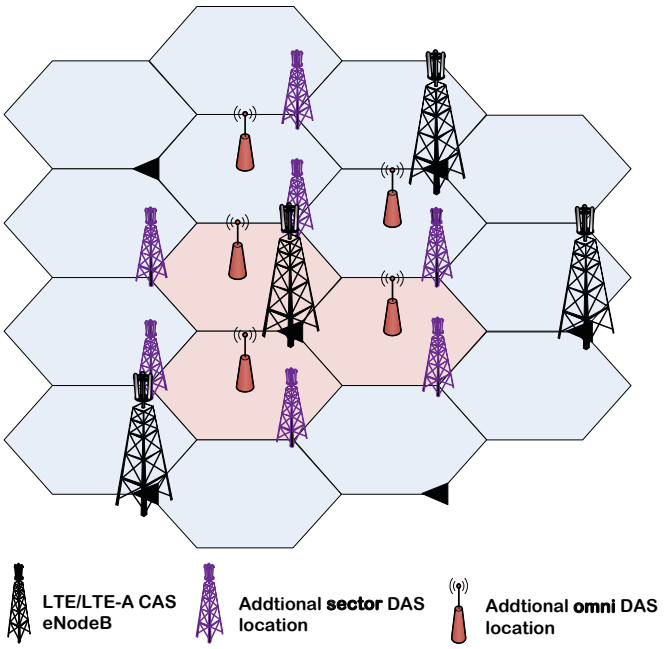

Figure 1. Heterogeneous network layout.

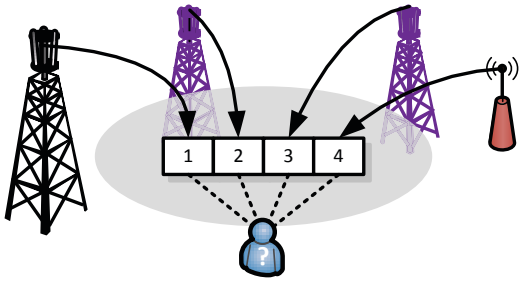

Figure 2. AS mode rank 1 with 4 selection possibilities for the UE inside of the serving cell.

B. Single Frequency Network

RRUs transmitting coherent on the the same radio frequency band to achieve a large coverage area are called single frequency network (SFN). For the following investigations we divide the possible single frequency network (SFN) transmission modes in rank 1 and rank 2 which means that either one or two independent data streams are active. Within a certain rank transmission the number of active antennas used for SFN can vary. Therefore, a dedicated transmission mode is denoted by rank m nSFN, where n is the number of antennas used for SFN[1] and m is the rank of the transmission. Note, that for rank 1 transmissions the rank indicator is omitted. Figure 3 shows 2 possible configurations of the 2 SFN transmission mode, while the UE is moving along a certain track.

[1]In our assumptions this means a coherent transmission of the same data symbol from these n antennas.

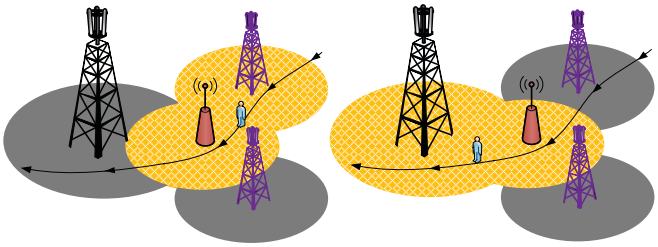

Figure 3. Illustration of a rank 2 SFN transmission switching transmit antennas adapting the actual UE locations on the user track.

C. LTE-dense

As described in Section II for LTE-dense we use the same RRU positions as in the DAS setting, but each location is equipped with a single BBU and all other equipment which is required for an eNodeB. Note, in contrast to a CAS deployment, each eNodeB will have its own cell-id. Thus, we increase the amount of cell-ids by a factor of four. The resulting cell densification is a well-known tool to increase peak data rates.

IV. Antenna Configuration

The DAS deployment that will be investigated in this work comprises three directional antennas and one omni-directional antenna. The deployment is illustrated in Figure 4(d) along with the indexing of the RRUs.

Recent simulations for system level investigations often use antenna patterns as stated in [7] which serves as a guideline for system level simulations. The proposed antenna pattern for a typical triple sectorized deployment is idealized generated to emulate real antennas. Figure 4 shows the directivity plots of the proposed patterns. Compared to practically deployed antennas such as the antenna 80010541 from KATHREIN this idealized antenna lacks the strong directivity in elevation direction. The Kathrein 80010541 has a half power beam width (HPBW) of about 6° compared to the 15° of the 3GPP 3D pattern. Therefore, to obtain realistic results we decided to employ a scheme as described in [9] to generate a three dimensional antenna pattern based on the KATHREIN 80010541. To focus the beam in the serving cell, the electrical tilt was put to 12°, the technical maximum of the KATHREIN antenna.

As stated in Section II, an omni-directional antenna is installed at the RRU4 in the center of the cell. In this work, we refrain from using an isotropic radiator as assumed in [7]. Using isotropic radiators for simulations creates unrealistic interference since it is an idealized antenna radiating equally in all directions which cannot be built in practice. Instead, we use the 80010442 from KATHREIN with the assumption that it would be electrically tilted by 12° like the KATHREIN 80010541. KATHREIN delivers the 80010442 with a fixed electric tilt of 0°. Technically, bar antennas can be electrically tilted like the KATHREIN 737546. We chose the 80010442 due to its small HPBW in elevation direction which is similar to the KATHREIN 80010541. Since the DAS deployment is

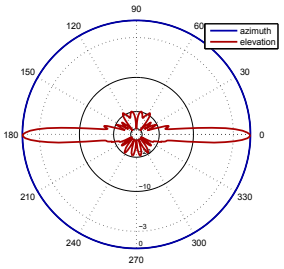

(a) KATHREIN 80010442

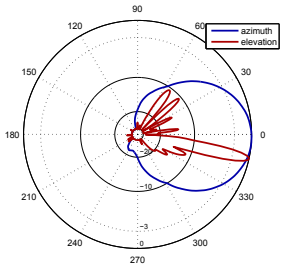

(b) KATHREIN 80010541

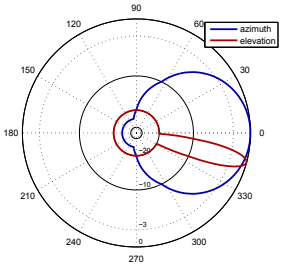

(c) 3GPP sector antenna

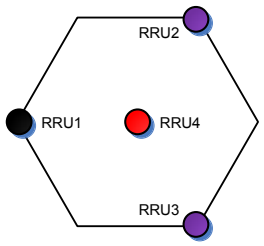

(d) DAS cell

Figure 4. Patterns of KATHREIN 80010442, 80010541 and 3GPP sector antenna pattern which were used in simulations and the RRU deployment in a single cell.

meant as an extension to an existing infrastructure RRU1 is put at a height of a standard urban macro base station according to [7]. The heights of RRU2-4 were chosen based upon the resulting distribution geometry and the received power for the investigated transmission concepts from section III. Varying the heights of the RRUs is another level to influence the interference condition in the cell in addition to the electrical tilt. In this work, we do not consider a mechanical tilting of the antennas. The heights were varied between 15m and 32m in 5m steps. The geometry and the received power distribution for varying heights of RRU2 and RRU3 in comparison to the case of all RRUs being installed at a height of 32m for the AS transmission concept is shown in Figure 5, where geometry corresponds to the ratio of receive power from the strongest to other antennas assuming that non selected antennas in the sector of interest are disabled. The heights were chosen as a compromise between the transmission concepts as well as a balance of the distribution and received power and geometry. The blue curve marks the height that was chosen for RRU2 and RRU3 if RRU4 is installed at a height of 15m. The geometry for LTE-dense and SFN behaved similarly although the heights can still be optimized if only one transmission concept would be utilized.

V. Downlink System Model

For a cellular orthogonal frequency division multiplex (OFDM) downlink system where the central site is surrounded by multiple tiers of sites, we assume each site to be partitioned into three 120° sectors, with a set $\mathcal{M}$ of $M = |\mathcal{M}|$ sectors in total. Each sector constitutes a cell id, and frequency resources are fully reused in all M sectors. The transmission on each

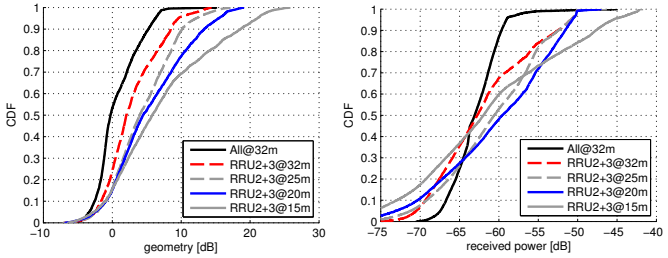

Figure 5. Geometry and received power in cell of interest for different heights of RRU2 and RRU3

subcarrier with N_t transmit antennas per base station (BS) and N_r receive antennas per UE is given by

$$\mathbf{y} = \mathbf{HBx} + \mathbf{n}, \tag{1}$$

where $\mathbf{H}$ denotes the $N_r \times N_t$ channel matrix, $\mathbf{B}$ the $N_t \times N_t$ pre-coding matrix, $\mathbf{x}$ the $N_t \times 1$ vector of transmit symbols and $\mathbf{y}$ the $N_r \times 1$ the received downlink signal. The $N_r \times 1$ vector $\mathbf{n}$ denotes the additive white Gaussian noise (AWGN) samples with covariance $\mathrm{E}\{\mathbf{nn}^H\} = \mathbf{I}\sigma_n^2$. The noise power comprises the receiver noise figure and the thermal noise power.

In general, each column of $\mathbf{B}_i$ can be seen as spatial transmission layer in the following denoted as $\mathbf{b}_{i,u}$, where i indicates the serving BS and u the spatial layer. With that the receive downlink signal $\mathbf{y}_k$ from BS i at UE k is given by

$$\mathbf{y}_k = \underbrace{\mathbf{H}_{i,k}\mathbf{b}_{i,u}\sqrt{p}_{i,u}}_{\overline{\mathbf{h}}_{i,u}} x_{i,u} + \underbrace{\sum_{\substack{j=1 \\ j\neq u}}^{N_t} \mathbf{H}_{i,k}\mathbf{b}_{i,j}\sqrt{p}_{i,j}x_{i,j}}_{\boldsymbol{\vartheta}_{i,u}} + \underbrace{\sum_{l\in\mathcal{M}\setminus i}\sum_{j=1}^{N_t}\mathbf{H}_{l,k}\mathbf{b}_{l,j}\sqrt{p}_{l,j}x_{l,j} + \mathbf{n}}_{\mathbf{z}_{i,u}}. \tag{2}$$

The effective channel from BS i to UE k is denoted as $\overline{\mathbf{h}}_{i,u}$. The distortion caused by surrounding BSs is divided into intra- and inter-sector interference aggregated in $\boldsymbol{\vartheta}_{i,u}$ and $\mathbf{z}_{i,u}$, respectively.

Assuming a linear equalizer $\mathbf{w}_{k,u}$ the achievable signal-to-interference-and-noise ratio (SINR) for layer u estimated at UE k can be expressed as

$$\mathrm{SINR}_{k,u} = \frac{\left|\mathbf{w}_{k,u}^H\overline{\mathbf{h}}_{i,u}\right|^2}{\left|\sum\limits_{\substack{j=1 \\ j\neq u}}^{N_t}\mathbf{w}_{k,u}^H\mathbf{H}_{i,k}\mathbf{b}_{i,j}\sqrt{p}_{i,j}\right|^2 + \left|\mathbf{w}_{k,u}^H\mathbf{z}_{i,u}\right|^2}. \tag{3}$$

Considering the DAS case intra-cell interference rejection combining (IRC) using the minimum mean square error (MMSE) receiver is possible [10] and leads to $\mathbf{w}_{k,u}^{\mathrm{MMSE}} = \mathbf{R}_{yy}^{-1}\overline{\mathbf{h}}_{i,u}$, where $\mathbf{R}_{yy}$ is the covariance matrix of the estimated received signals combined in $\mathbf{y}_k$.

$$\mathbf{R}_{yy} = \boldsymbol{\vartheta}_{i,u}\boldsymbol{\vartheta}_{i,u}^H + \mathrm{trace}(\mathbf{z}_{i,u}\mathbf{z}_{i,u}^H) + \overline{\mathbf{h}}_{i,u}\overline{\mathbf{h}}_{i,u}^H. \tag{4}$$

In the LTE-dense case the number of sectors is $M_{\text{dense}} = MN_t$, where $N_{t,\text{dense}}$ denotes the number of transmit antennas per BS in the LTE-dense case and is set to one. This results in $\vartheta_{i,u} = 0$ which means that all interference is seen as inter-sector interference. The estimated covariance matrix of the applied MMSE equalizer becomes

$$\mathbf{R}_{yy} = \text{trace}(\mathbf{z}_{i,u}^{\text{dense}}[\mathbf{z}_{i,u}^{\text{dense}}]^H) + \overline{\mathbf{h}}_{i,u}\overline{\mathbf{h}}_{i,u}^H, \qquad (5)$$

where $\mathbf{z}_{i,u}^{\text{dense}}$ denotes the inter-sector interference for the LTE-dense case. From 5 it can be seen that distortion from other BSs is seen as inter-cell interference which leads directly to $\text{SINR}_u^{\text{DAS}} \geq \text{SINR}_u^{\text{dense}}$.

VI. Numerical Simulation Results

A. Simulation Assumptions

The network deployment was described in general in Section II. All parameters and assumptions which are not explicitly explained are summarized in the upper part of Table I. Setting details of the underlying channel model are listed in the lower part.

The upper part of Table II summarizes the configuration at eNodeB. In Section IV the details of antennas are already discussed. On UE side we assume two vertical polarized omni-directional receive antennas. The complete UE configuration is listed in lower part of Table II. Extensive informations of the score-based scheduler can be found in [11]. Note, that the global scheduling goal is to assign each user an equal amount of its best resources. The number of statistically independent simulation runs is set to 500.

Table I
Network layout and channel setting

Network layout	
Number of sectors	57
Sector type	120
CAS ISD	500 m
Spatial layer support	up to 4
Frequency reuse	1
Duplex mode	FDD
Minimum distance to eNodeB	35 m
UE distribution	Uniform
Number UEs per sector	10
Channel settings	
Carrier frequency	2.6 GHz
Path-loss model [dB]	17.75 + 37.6 * log10(distance [m])
Additional penetration loss	20 dB
Time resolution	1 ms
Number of subframes	200
Mobility	3 km/h
Bandwidth	20 MHz
Frequency resolution	180 kHz
Number of RE per RB	168
Small scale fading	SCME
Scenario	Urban-macro
Shadow Fading (SF) model	log-normal
SF intra-site correlation	1
SF inter-site correlation	None
SF standard deviation	8 dB
SF correlation distance	Spatially i.i.d.

Table II
Configuration at eNodeB and UE.

Configuration at eNodeB	
Number transmit antennas	4 vertical polarized
Total transmit power	46
Transmit power distribution	Equal per RB
Antenna model	3GPP 2D, 3D or Katrein
Electrical down-tilt	12 & 15 degrees
Antenna heights	
CAS	32 m
Additional sector antenna	20 m
Additional omni antenna	15 m
Scheduling	Score-based in space, frequency and time
Configuration at UE	
Number receive antennas	2 vertical polarized
Antenna model	Omni-directional
Cell selection	Maximum received power based on PSS
CQI generation	EESM
CQI reporting	interval 1 ms
Subband size	8 (last subband 4)
TBLER	0.1
PMI generation	based on maximum received power
Feedback delay	0 ms
Channel estimation	Perfect
Receive filters	MMSE
Noise figure	9 dB
AWGN	Thermal noise with -174 dBm/Hz
HARQ	Not supported

B. Performance Evaluation

Figure 6 shows the system throughput of the different antenna models for the LTE CAS scenario. It is noticeable that the median value increases from the 3GPP 2D to the KATHREIN antenna model by more than 15%. This confirms that realistic antenna modeling has a significant impact and has to be considered as explained in Section IV.

A comparison of the SFN and AS modes with the baseline scenario LTE-CAS is shown in Figure 7. We observe an parallel shifting of the cumulative distribution function (CDF) curve from LTE-CAS to 2SFN and to AS rank 1 of 14 and 21%, respectively. The higher variance of the 4SFN mode with a median value of 47 Mbit/s is caused by the coherent

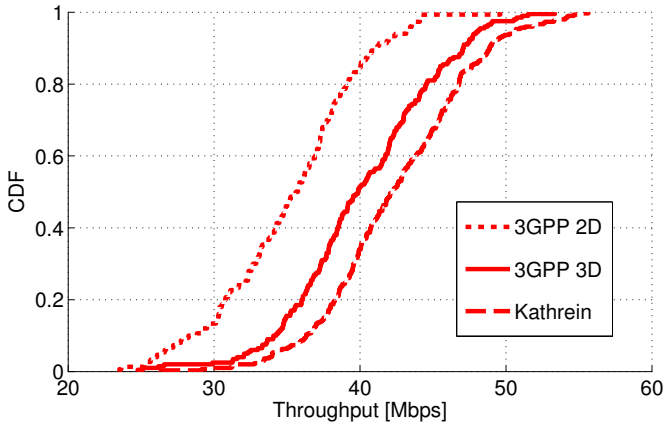

Figure 6. LTE-CAS rank 1 transmission comparing different antenna patterns.

transmission from four antennas. This means UEs located in the middle of the sector are experiencing higher SINR than for example 2SFN and lower SINR at the border because all antennas from neighbor sectors are also active. Therefore, the level of inter-cell interference is higher compared to AS or 2SFN where only one respectively 2 antennas are active. Note, that LTE CAS and 4SFN have the same total sum output power of 46 dBm. As illustrated in Figure 3 for 2SFN an adaptive switching of the active antennas can cover different areas inside the sector which leads to a steeper curve with half of the power consumption of the 4SFN mode. The AS mode has the highest throughput at the median due to the adaptive antenna switching where only a fourth of all antennas is active leading to a lower level of inter-cell interference than for other modes. Therefore, the transmit power is also a fourth compared to LTE-CAS.

As a next step, we increase the transmission rank up to 3.

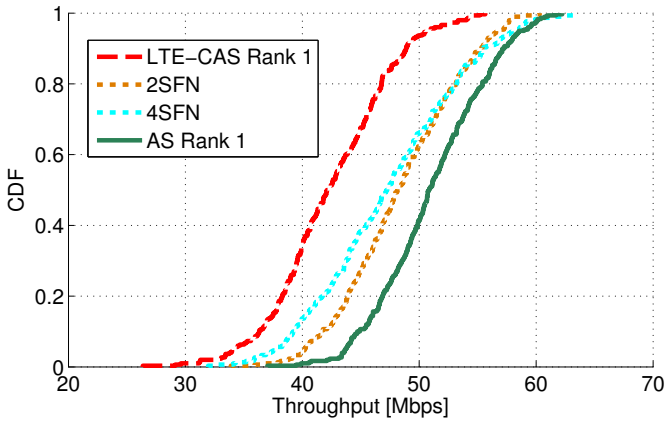

Figure 7. DAS Rank 1 with AS and SFN transmission mode compared to LTE CAS

A special focus is put on the reduction of feedback overhead by limiting the number of reported precoding matrix indicator (PMI) values. For rank 2, 6 PMIs and for rank 3, 4 PMIs exist. To limit the number of reported PMIs only the strongest PMIs in terms of receive power based on a broadband estimation are selected for feedback. In Figure 8(a) the system performance degradation by allowing only a single PMI (sPMI) value can be exploited which is 25% compared to multi PMI where 6 PMI values are reported. The rank 2 2SFN mode has 40 Mbit/s at the median value which is 60% of the performance from rank 2 sPMI. The required feedback can be further reduced by limiting the number of channel quality indicator (CQI) values reported per PMI which is shown for rank 3 in Figure 8(b). First the feedback is reduced from full to sPMI again causing a degradation of 20% and from this straightforward to a single CQI value. It is noticeable, that the reduction from 3 to 2 streams causes approximately no loss in system throughput. The explanation for this is the number of receive antennas on UE side which is set to 2. This limits the number of streams which can be separated at the receiver also to 2, therefore it is sufficient to report the 2 strongest CQI per PMI. By further reducing CQI reporting to a single data stream, scheduling becomes more difficult. Since the scheduling entity has to find three different UEs reporting for the same PMI but for different data streams, the sector throughput decreases by approximately 7%.

Finally, transmission with rank 4 is taken into account.

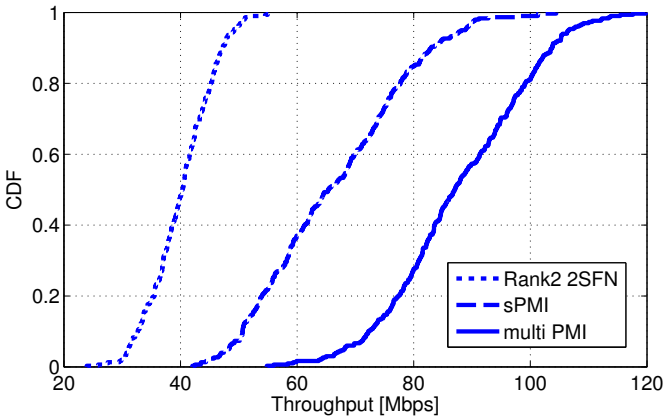

(a) Rank 2

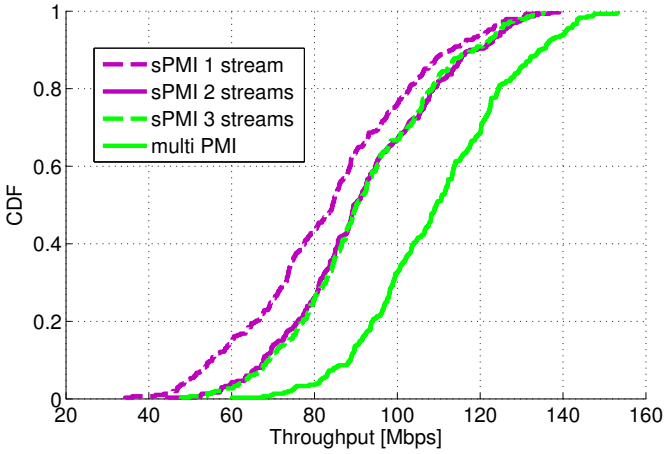

(b) Rank 3

Figure 8. Antenna selection with feedback reduction.

There is only a single PMI for full rank so that no feedback reduction is shown. In Figure 9 the system throughput for LTE-CAS rank 1, AS rank 1 to 4 and LTE-dense for an overall comparison is depicted. Note, that only AS rank 4 has the same resource reuse factor over area as LTE-dense. Considering full buffer assumption at UE side it becomes clear that LTE-dense has a higher throughput at the median value than AS rank 3. Due to the intra-cell interference suppression as explained in Section V AS rank 4 outperforms LTE-dense.

VII. Conclusions & Discussion

Within this paper, we evaluated the system performance of a DAS layout fully compatible with a standard LTE scenario and demonstrated that it is capable to outperform the LTE-CAS or LTE-dense system in multiple ways. As shown in Section VI a performance gain for rank 1 transmission

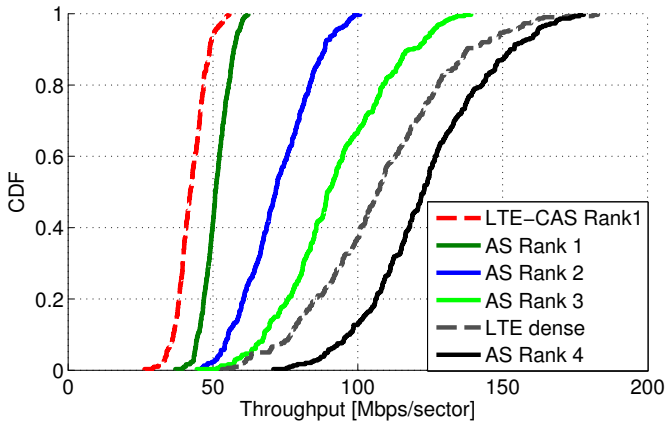

Figure 9. Transmission mode comparison

with 0.25 of the power consumption from the LTE-CAS can be achieved by smarter placement of RRUs.

Compared to the LTE-dense system, DAS involves less hardware, 4 RRUs and 1 BBU instead of 4 RRUs and 4 BBUs. Because of a larger cell size, fewer handovers are required for mobile users, since the DAS scenario uses the same cell-id for all 4 RRUs. These advantages are achieved by the requirement of a backhaul connection with low latency and high capacity as well as more signaling overhead. The installation costs of new RRUs are the same for DAS and LTE-dense.

Assuming full buffer, an increase in peak, median and cell edge data rate is achieved due to intra-cell IRC since sub-channels of the same cell id can be estimated, as explained in Section V. Not explicitly shown in this paper but nonetheless an important issue is the higher flexibility of the DAS by transmission mode switching to adapt to changing user requirements. These changes arise for example due to non-uniform user distributions, called user hot spots, or by modeling realistic user traffic instead of full buffer. Especially the AS rank 3 mode is a potential candidate to adapt to such changes which achieves similar system performance as LTE-dense with 25% less power consumption and the capability of shifting interference zones.

The SFN mode should be selected for users with higher mobility, since those users will benefit from the fact that the coverage in a certain location is more homogeneous.

The antenna selection modes are very beneficial in application where multiple UEs can be served within the same time and frequency slot but on different spatial layers. Each UE would select a certain PMI dependent on its location and desired selection strategy. For future investigation, it would be very promising to study different methodology in selection of PMIs, which are not limited to maximum received power.

REFERENCES

[1] Cisco, "Global Mobile Data Traffic Forecast Update, 2011-2016," *Cisco white paper*, vol. 1, p. 29, 2012.

[2] 3GPP, "Improvements of distributed antenna for 1.28 Mcps TDD," 3rd Generation Partnership Project, Tech. Rep., Dec 2010.

[3] R. Heath, T. Wu, Y. H. Kwon, and A. Soong, "Multiuser MIMO in Distributed Antenna Systems With Out-of-Cell Interference," *Signal Processing, IEEE Transactions on*, vol. 59, no. 10, pp. 4885 –4899, Oct 2011.

[4] W. Choi and J. Andrews, "Downlink performance and capacity of distributed antenna systems in a multicell environment," *Wireless Communications, IEEE Transactions on*, vol. 6, no. 1, pp. 69 –73, jan. 2007.

[5] H. Dai, "Distributed Versus Co-Located Mimo Systems with Correlated Fading and Shadowing," in *Acoustics, Speech and Signal Processing, 2006. ICASSP 2006 Proceedings. 2006 IEEE International Conference on*, vol. 4, May 2006, p. IV.

[6] Y. Yu and D. Gu, "Enhanced MU-MIMO Downlink Transmission in the FDD-Based Distributed Antennas System," *Communications Letters, IEEE*, vol. 16, no. 1, pp. 37 –39, Jan 2012.

[7] ITU, "Guidelines for evaluation of radio interface technologies for IMT-Advanced," ITU - International Telecommunication Union, Tech. Rep., 2008.

[8] 3GPP, "Further advancements for E-UTRA physical layer aspects," 3rd Generation Partnership Project, Tech. Rep. Release 9, Mar 2010.

[9] L. Thiele, T. Wirth, K. Börner, M. Olbrich, V. Jungnickel, J. Rumold, and S. Fritze, "Modeling of 3D Field Patterns of Downtilted Antennas and Their Impact on Cellular Systems," in *International ITG Workshop on Smart Antennas (WSA 2009)*, Berlin, Germany, Feb 2009.

[10] J. Winters, "Optimum Combining in Digital Mobile Radio with Cochannel Interference," *IEEE Journal on Selected Areas in Communications*, vol. 2, no. 4, pp. 528–539, Jul 1984.

[11] M. Schellmann, L. Thiele, V. Jungnickel, and T. Haustein, "A Fair Score-Based Scheduler for Spatial Transmission Mode Selection," in *Signals, Systems and Computers, 2007. ACSSC 2007. Conference Record of the Forty-First Asilomar Conference on*, Pacific Grove, CA, Nov 2007, pp. 1961–1966.